PACS numbers: 42.55. Lt
DOI: 10.1070/QE2009v039n05ABEH013974

An improved model of gas temperature in a copper bromide vapour laser

I.P. Iliev, S.G. Gocheva-Ilieva, N.V. Sabotinov

***Abstract*. A new analytic model is proposed for calculating the temperature profile of gas in the transverse section of the discharge tube of copper bromide lasers emitting at 510.6 and 578.2 nm. The model is described by the quasi-stationary heat conduction equation with the boundary conditions of the third and fourth kinds taking into account the alternating volume electric power along the tube radius. The exact solution of the problem is obtained. The model was used to calculate the temperature profiles of the discharge in the case of natural and forced convection cooling. The obtained results are compared with previously known temperature distributions. The improved model proposed in the paper can be used to analyse existing lasers and develop new lasers.**

Keywords: *copper bromide laser, temperature model, heat conduction equation, exact solution.*

1. Introduction

Although at present the most popular are semiconductor lasers, copper and copper compound vapour lasers still find a variety of applications. They are the highest-power radiation sources in the visible spectral region at 510.6 and 578.2 nm, emit highly coherent and low-divergence beams and also can be used as UV radiation sources emitting at 248.6, 259.2, 260.0, and 270.3 nm. For these reasons copper vapour lasers remain the object of experimental and theoretical studies [1–7]. Experiments with such lasers and their operating conditions show that the gas temperature in the active laser medium is one of their most important operation parameters. Thus, a detailed study of the gas temperature distribution in the active-medium cross section is very important both for existing copper vapour lasers and the development of new lasers.

So far the gas temperature distribution $T_g(r)$ in the laser tube cross section in all the analytic models of copper and copper compound vapour lasers [8–10] was described by the expression

$$T_g(r) = \left[T_1^{m+1} + \frac{q_v(m+1)}{4\lambda_0}(R_1^2 - r^2)\right]^{1/(m+1)}, \quad 0 \leqslant r < R_1, \tag{1}$$

where R_1 and T_1 are the radius and temperature of a quartz tube; q_v [W m^{-3}] is the volume electric power released in the active medium; and λ_0 and m are constants depending on the gas type.

Expression (1) is also applied to simulate gas temperature distributions in lasers based on other metal compounds [11]. It is valid if the power q_v is constant in the entire active-medium volume. However, this assumption does not correspond to the real distribution of q_v in the laser-tube cross section. It is known that q_v strongly changes along the tube radius, and the maximum power is localised on the discharge axis. Thus, the use of expression (1) under condition $q_v = \text{const}$ is incorrect, and it can be employed only for qualitative and comparative estimates of the gas temperature in the laser tube cross section. A more accurate method is required to perform real calculations of temperature distributions.

In this paper, we studied analytically the temperature profile in the cross section of a laser tube when the distribution of the volume electric power along the tube radius was specified in advance: $q_v = q_v(r)$. Such an approach allows us to find the temperature distribution in the active medium of a laser more accurately than expression (1). This study is in fact the continuation and development of our previous paper [10]. Thus, we first briefly present the main results obtained in [10].

2. Analytic model developed in [10]

We will study a copper bromide vapour laser [12]. Let us assume that the total electric power consumed by the laser is 5000 W. Taking losses into account, the power $Q_1 = 4080$ W is supplied to the active volume of the laser, and the output power is 120 W. The dimensions of the laser tube are shown in Fig. 1. The tube is made of quartz and has an additional heat-insulating cover made of glass wool, mineral wool or zirconium dioxide wool.

I.P. Iliev Department of Physics, Technical University, Plovdiv, 25, Tzanko Djusstabanov St., 4000 Plovdiv, Bulgaria;
e-mail: iliev55@abv.bg;
S.G. Gocheva-Ilieva Department of Applied Mathematics and Modelling, Faculty of Mathematics and Informatics, Paisii Hilendarski Uiversity of Plovdiv, 24 Tzar Assen St., 4000 Plovdiv, Bulgaria;
e-mail: snow@uni-plovdiv.bg, snegocheva@yahoo.com;
N.V. Sabotinov Metal Vapour Lasers Department, Georgy Nadjakov Institute of Solid State Physics, Bulgarian Academy of Sciences, 72, Tsarigradsko Chaussee, 1784 Sofia, Bulgaria;
e-mail: nsabotinov@issp.bas.bg

Received 22 September 2008
Kvantovaya Elektronika **39** (5) 425–430 (2009)
Translated by M.N. Sapozhnikov

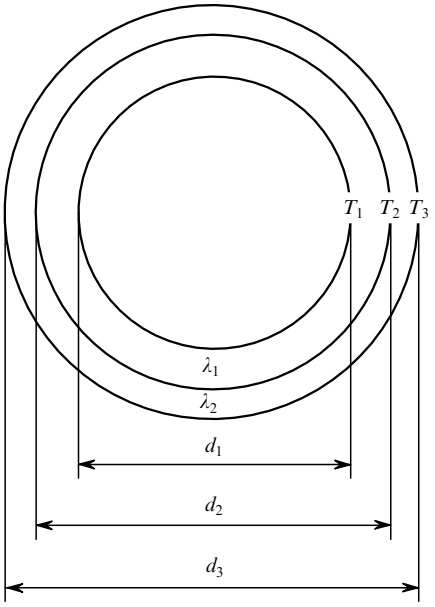

Figure 1. Cross section of a copper bromide laser tube in the active-medium volume. The internal diameter of the quartz tube is $d_1 = 60$ mm, the external diameter is $d_2 = 64$ mm, the external diameter of the heat-insulating cover is $d_3 = 74$ mm.

The temperature profile was simulated by assuming that [10]: (i) the temperature profile of a discharge is determined in the quasi-stationary operation regime of the laser; (ii) the gas temperature between excitation pulses changes insignificantly; (iii) all the electric power (4080 W) supplied to the active volume is transformed in it to the thermal energy, and power transferred to the tube walls due to discharge emission and deactivation of excited and charged particles on the walls is neglected.

By using the additional assumption that $q_v = \text{const}$, we developed in [10] the following analytic model. The gas temperature T_g in the laser tube cross section was determined by solving the two-dimensional steady-state heat conduction equation

$$\operatorname{div}(\lambda \operatorname{grad} T_g) + q_v = 0, \tag{2}$$

where λ is the heat conductivity of gas. Equation (2) was solved by using mixed boundary conditions of the third and fourth kinds in a cylindrical configuration:

$$T_1 = T_2 + \frac{q_l \ln(d_2/d_1)}{2\pi\lambda_1}, \quad T_2 = T_3 + \frac{q_l \ln(d_3/d_2)}{2\pi\lambda_2}, \tag{3a}$$

$$Q_1 = \alpha F_3 (T_3 - T_0) + F_3 \varepsilon c \left[\left(\frac{T_3}{100} \right)^4 - \left(\frac{T_0}{100} \right)^4 \right], \tag{3b}$$

where T_1, T_2, and T_3 are temperatures on the tube walls and heat-insulating cover, respectively (Fig. 1); $q_l = Q_1/l_a$ is the released thermal power per unit length; $l_a = 2$ m is the active length of the laser; λ_1 and λ_2 are the heat conductivities of the quartz tube and heat insulation, respectively; $d_{1,2,3}$ are tube diameters (Fig. 1); $Q_1 = 4080$ W is the total heat release equal to the consumed electric power (according to the third assumption); α is the coefficient of heat transfer from the external surface of the heat-insulating cover to the environment; F_3 is the external surface area of the heat-insulating cover; $c = 5.67$ W m^{-2} K^{-4} is the emission coefficient of the perfectly black body; $T_0 = 300$ K is the air temperature; and ε is the integrated degree of blackness of the heat-insulating cover.

The values of parameters used in calculations are presented in Table 1. Equations (2), (3a), and (3b) were solved in [10] by using (1) and assuming that $q_v = \text{const}$.

3. Determination of the gas temperature taking the radial distribution of the volume power into account

3.1 Determination of the radial distribution $q_v = q_v(r)$

Because reliable experimental data on the dependence of the volume power q_v on the parameter r are not available, we will use some qualitative theoretical dependences. From the relation $q_v = jE$ and $j \approx \sigma E$, where j is the current density and σ is the conductivity, we obtain $q_v \approx \sigma E^2$. According to [13], the distribution of the electric field strength E in the tube cross section is described by the expression $E(r) = E_0 J_0(2.4r/R_1)$, where $J_0(2.4r/R_1)$ is the Bessel function of the first kind of the zeroth order. Then,

$$q_v(r) = Q \left[J_0 \left(\frac{2.4}{R_1} r \right) \right]^2, \tag{4}$$

where Q is an unknown constant, which should be determined. The function $J_0(2.4r/R_1)$ is well known and tabulated, for example, in [14]. Because manipulations with the Bessel function in the general case are inconvenient, we will use the approximate relation $[J_0(x)]^2 = a + bx + cx^2 + dx^3$. We will set for convenience $x = 2.4r/R_1 = \beta r$; $\beta = 2.4/R_1$. Then, by using tabulated data from [14], we find by the method of least squares that $a = 1.0044$, $b = -0.01768$, $c = -0.5657$, and $d = 0.1668$. This gives

$$q_v(r) = Q[a + b\beta r + c(\beta r)^2 + d(\beta r)^3]. \tag{5}$$

To obtain the constant Q, we will use the equality of areas under the plots of functions $q_v = q_0 = \text{const}$ and $q_v = q_v(r)$ (Fig. 2):

$$2q_0 R_1 = 2Q \int_0^{R_1} (a + Br + Cr^2 + Dr^3) \mathrm{d}r. \tag{6}$$

Here, we assume for simplicity that

Table 1. Data used to calculate the temperature profile [10].

Q_1/W	l_a/m	q_v/W cm^{-3}	q_l/W m^{-1}	$\lambda_g = \lambda_0 T_g^m$/W m^{-1} K^{-1}	λ_1/W m K^{-1}	λ_2/W m K^{-1}	ε
4080	2	0.7219	2040	$\lambda_0 = 5.8935 \times 10^{-5}$ ($m = 1.091$, $p_{Ne} = 15$ Torr, $p_{H_2} = 0.3$ Torr)	1.96 ($T = 800 - 1100$ K)	0.12 ($T = 800 - 1100$ K, mineral insulation)	0.72

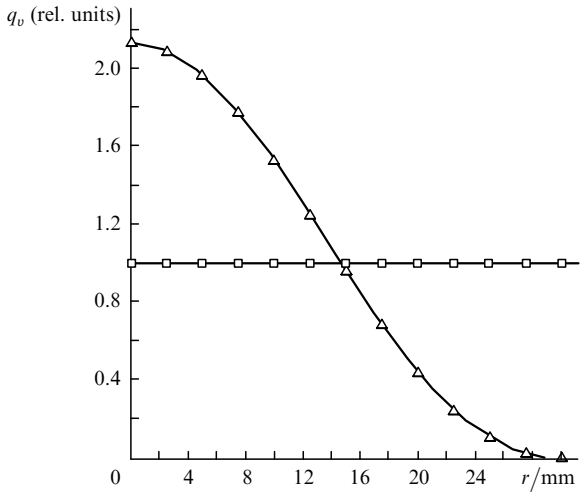

Figure 2. Distribution of the volume power density in the laser tube cross section: (□) $v = q_0 = 1$, (△) $q_v = q_v(r)$ [expression (5)].

$$B = b\frac{2.4}{R_1},\ C = c\left(\frac{2.4}{R_1}\right)^2,\ D = d\left(\frac{2.4}{R_1}\right)^3. \tag{7}$$

After integration in (6), we obtain

$$Q = q_0\left(a + \frac{b}{2}2.4 + \frac{c}{3}2.4^2 + \frac{d}{4}2.4^3\right)^{-1}. \tag{8}$$

Now, by substituting the values of constants a, b, c, and d, we find

$$Q = 2.131 q_0. \tag{9}$$

For comparison, Fig. 2 shows distributions $q_v = q_0 = \text{const}$ and $q_v = q_v(r)$ calculated by (5) and (9) (we set conditionally $q_0 = 1$). One can see from Fig. 2 and (9) that the local electric power released at the discharge centre in the case of distribution (5) is twice that for $q_v = \text{const}$. This suggests that temperature distributions $T_g(r)$ in the discharge in the cases $q_v = \text{const}$ and $q_v = q_v(r)$ are substantially different.

3.2 Determination of the discharge temperature $T_g(r)$

The exact solution of equations (2) and (3) with radial distribution (5) has the form

$$T_g(r) = \left\{T_1^{m+1} + \frac{(m+1)Q}{\lambda_0}\left[\frac{a}{4}(R_1^2 - r^2) + \frac{B}{9}(R_1^3 - r^3) + \frac{C}{16}(R_1^4 - r^4) + \frac{D}{25}(R_1^5 - r^5)\right]\right\}^{1/(m+1)}, \tag{10}$$

where $B = b(2.4/R_1), C = c(2.4/R_1)^2, D = d(2.4/R_1)^3$. The solution of (10) is obtained in Appendix.

4. Application of the model for determining the temperature profile in the discharge tube cross section and analysis of results

Similarly to [10], we will seek the temperature distribution $T_g(r)$ by using analytic model (2), (3) for the cases of discharge cooling either by natural or forced convection. For thus purpose, we will use additional data from Table 1 [10].

Expression (10) can be used if the temperature T_1 of the inner wall of the quartz tube is known (Fig. 1). Two cases are possible:

(i) The temperature T_2 of the external wall of the quartz tube inside the insulating layer is known. This temperature can be measured in real lasers, for example, by using a thermocouple, and then T_1 can be determined from (3a).

(ii) Temperatures T_2 and T_3 are unknown. In particularly, this is the case in the development of new lasers. In this case, model (2), (3) can be used with boundary condition (3b), where the environmental temperature is specified usually as $T_0 = 300$ K. By solving nonlinear equation (3b), we find T_3 and then determine T_2 and T_1 from (3a).

We considered in [10] the second case. Here, we will study the same case and compare the results with data obtained in [10].

To determine T_3 from boundary condition (3b), it is necessary to find preliminarily the heat-transfer coefficient α. Consider the cases of cooling due to natural and forced convection.

4.1 Natural convection

Condition (3b) in [10] in the case of natural convection is written in the form

$$q_l = 0.46\pi\lambda_{\text{air}}\left(g\beta_{\text{air}}d_3^3\frac{T_3 - T_0}{\nu_{\text{air}}^2}\right)^{0.25}(T_3 - T_0) + \pi d_3\varepsilon c\left[\left(\frac{T_3}{100}\right)^4 - \left(\frac{T_0}{100}\right)^4\right], \tag{11}$$

where g is the gravitational acceleration; β is the volume thermal expansion coefficient of gas (for air, $\beta_{\text{air}} = 3.41\times 10^{-3}$ K^{-1}); ν is the kinematic viscosity ($\nu_{\text{air}} = 15.7\times 10^{-6}$ m^2 s^{-1}); and λ is the heat conductivity ($\lambda_{\text{air}} = 0.0251$ W m^{-1} K^{-1}).

In (11), only the temperature T_3 is unknown. It is found by solving this nonlinear equation, and then T_2 and T_1 are calculated from (3a) and $T_g(r)$ is determined from (10).

Figure 3 presents temperature distributions $T_g(r)$ for $q_v = q_0 = \text{const}$ and $q_v = q_v(r)$. Temperatures T_3, T_2 and

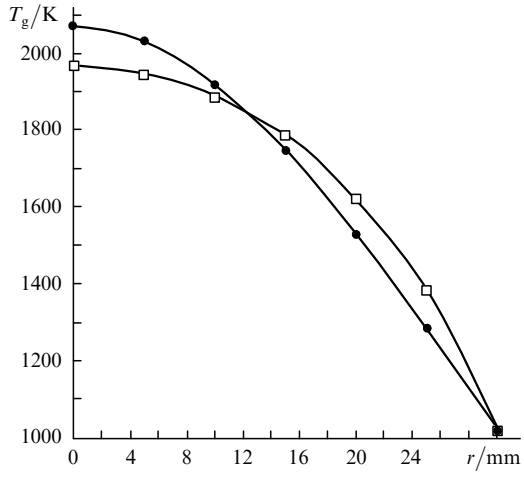

Figure 3. Distribution of the gas temperature in the laser tube cross section during natural convection. The supplied power is $Q_1 = 4080$ W. (□) $q_v = q_0 = \text{const}$, (●) $q_v = q_v(r)$.

Table 2. Temperature at characteristic points (Fig. 1) during natural convection.

Power distribution	T_3/K	T_2/K	T_1/K	$T(0)$/K
$q_v = q_0 = \text{const}$	617	1010	1021	1967
$q_v = q_v(r)$	617	1010	1021	2070

T_1 calculated at characteristic points and the maximum temperature $T(0)$ achieved at the tube centre are presented in Table 2.

One can see from Table 2 that for $q_v = q_0 = \text{const}$ and $q_v = q_v(r)$, temperatures T_3, T_2, and T_1 are identical. Their values are determined by the total electric power released in the active volume and are independent of its radial distribution. In the two cases under study, this power is the same (4080 W). Table 2 and Fig. 3 also show that temperature $T(0)$ for the distribution $q_v = q_v(r)$ is higher by 100 °C than $T(0)$ for $q_v = \text{const}$.

4.2 Forced convection

In this case, as shown in [10], boundary condition (3b) can be written in the form

$$q_l = 0.615\pi\lambda_{\text{air}}\left(\frac{\upsilon d_3}{\nu_{\text{air}}}\right)^{0.466}(T_3 - T_0)$$

$$+\pi d_3\varepsilon c\left[\left(\frac{T_3}{100}\right)^4 - \left(\frac{T_0}{100}\right)^4\right], \qquad (12)$$

where υ is the velocity of the cooling (forced) air flow.

The temperature T_3 can be determined from equation (12) and then by using (3a) and (10), we can find the temperature profile and in the discharge tube cross section.

Table 3 presents characteristic temperatures T_3, T_2, and T_1. The distribution $T_g(r)$ is shown in Fig. 4. In both cases, calculations were performed for the flow rate $\upsilon = 20$ m s^{-1}.

Table 3. Temperature at characteristic points (Fig. 1) during forced convection.

Power distribution	T_3/K	T_2/K	T_1/K	$T(0)$/K
$q_v = q_0 = \text{const}$	466	858	881	1903
$q_v = q_v(r)$	466	858	881	2009

As in the case of natural convection, temperatures T_3, T_2, and T_1 for $q_v = \text{const}$ and $q_v = q_v(r)$ are the same, respectively. Note that in the case of forced convection, $T(0)$ for the distribution $q_v = q_v(r)$ is higher by 100 °C than $T(0)$ for $q_v = \text{const}$.

4.3 Analysis of simulation results

Although, according to Fig. 2, the maximum electric power at the tube centre in the case of $q_v = q_v(r)$ is twice that in the case of $q_v = q_0 = \text{const}$, the corresponding temperatures $T(0)$ for natural and forced convection differ only by 100 °C. Thus, in both cases the ratio $\Delta T(0)/T_{q_v(r)}(0)$ is 5.1 %, on average, and hence, solution (1) can be applied to analyse the temperature regime of laser sources.

However, the absolute difference of temperatures at the discharge centre equal to 100 °C cannot be neglected. Expression (10) better explains and predicts the appearance of a number of negative effects caused by the overheating of the laser medium. An increase in the temperature at the tube centre by 100 °C can lead to the compression of a gas discharge, the thermal-ionisation instability, the thermochemical degradation of gas and to the additional thermal population of lower laser levels. Finally, this will lead to a decrease in the laser radiation power and the impairment of its mode composition. In some cases, the discharge overeating at the tube centre can initiate the quenching of lasing and the appearance of dark spots at the laser beam centre. For this reason, despite the complicate form of expression (10), it can be recommended for applications.

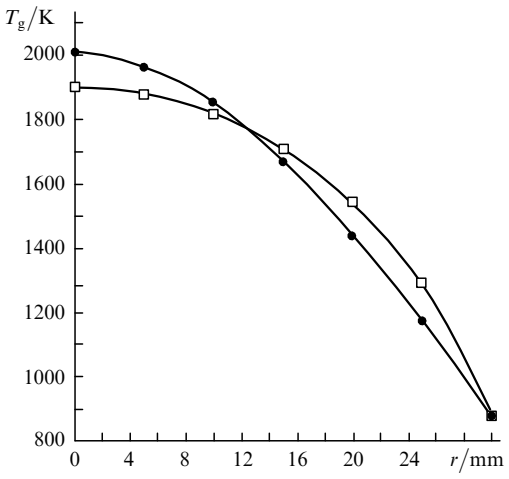

Figure 4. Distribution of the gas temperature in the laser tube cross section during forced convection. The supplied power is $Q_1 = 4080$ W. (□) $q_v = q_0 = \text{const}$, (●) $q_v = q_v(r)$.

5. Conclusions

The analytic model has been proposed for determining the gas temperature, which takes into account the nonuniform distribution of the electric power in the laser-tube cross section.

Based on the most general theoretical dependences, the distribution of the volume density of the electric power in the tube cross section of the type $q_v = q_v(r)$ is proposed [expression (5)].

The heat conduction equation is solved for cases of natural and forced convection and explicit analytic expressions are obtained which describe the gas temperature distribution $T_g(r)$ under these conditions.

It is shown that the distribution $T_g(r)$ obtained earlier assuming that $q_v = \text{const}$ gives the calculation error of $T_g(r)$ at the tube centre ~ 5 %. The temperature profiles obtained for $q_v = \text{const}$ and $q_v = q_v(r)$ are compared. It is found that the gas temperature at the tube centre for $q_v = q_v(r)$ is higher by 100 °C than that for $q_v = \text{const}$. Analysis of the results has shown that such elevated temperature can considerably affect the discharge behaviour. A new expression for determining $T_g(r)$ is proposed.

Acknowledgements. This work was supported by the National Scientific Fund of the Bulgarian Ministry of Education and Science (Grant No. VU-MI-205/2006) and the Paisii Hilendarski Plovdiv University (Grant No. RS-FMI-013).

Appendix

Let us solve the heat conduction equation

$$\mathrm{div}(\lambda \mathrm{grad} T_\mathrm{g}) + q_v = 0, \tag{A1}$$

where λ is the heat conductivity of gas and q_v is the volume density of released power.

The quartz tube wall temperature and the axial symmetry of the temperature distribution in the active medium are specified by the boundary conditions

$$T_\mathrm{g}(R_1) = T_\mathrm{w}, \tag{A2}$$

$$\left.\frac{\mathrm{d}T_\mathrm{g}}{\mathrm{d}r}\right|_{r=0} = 0. \tag{A3}$$

In cylindrical coordinates in the case of the axial and longitudinal symmetry, equation (A1) can be written in the form

$$\frac{1}{r}\frac{\mathrm{d}}{\mathrm{d}r}\left(r\lambda\frac{\mathrm{d}T_\mathrm{g}}{\mathrm{d}r}\right) + q_v = 0. \tag{A4}$$

The heat conductivity is usually represented in the form

$$\lambda(r) = \lambda_0 T_\mathrm{g}^m,$$

where λ_0 and m are constants depending on the gas type. Thus, equation (A4) takes the form

$$\frac{1}{r}\frac{\mathrm{d}}{\mathrm{d}r}\left(r\lambda_0 T_\mathrm{g}^m\frac{\mathrm{d}T_\mathrm{g}}{\mathrm{d}r}\right) + q_v = 0. \tag{A5}$$

After the substitution of the variable

$$U(r) = T_\mathrm{g}^{m+1} \tag{A6}$$

equation (A5) takes the form

$$\frac{\mathrm{d}^2U}{\mathrm{d}r^2} + \frac{1}{r}\frac{\mathrm{d}U}{\mathrm{d}r} + \frac{q_v(m+1)}{\lambda_0} = 0, \tag{A7}$$

and boundary conditions take the form

$$U(R_1) = T_\mathrm{w}^{m+1}, \tag{A8}$$

$$\frac{\mathrm{d}U}{\mathrm{d}r}|_{r=0} = 0. \tag{A9}$$

For $q_v = q_0 = \mathrm{const}$, the solution of equation (A7) is

$$U(r) = U_\mathrm{w} + \frac{q_0(m+1)}{4\lambda_0}(R_1^2 - r^2).$$

Taking (A6) and (A8) into account, we obtain known expression (1) [8–11]

$$T_\mathrm{g}(r) = \left[T_\mathrm{w}^{m+1} + \frac{q_0(m+1)}{4\lambda_0}(R_1^2 - r^2)\right]^{1/(m+1)}.$$

To solve equation (A7) for $q_v = q_v(r)$, we introduce a new variable

$$\tau = \frac{\mathrm{d}U}{\mathrm{d}r}. \tag{A10}$$

Equation (A7) can be written in the form

$$\mathrm{d}(r\tau) + \frac{m+1}{\lambda_0}q_v r\mathrm{d}r = 0.$$

By integrating this equation taking (5) and (7) into account, we obtain

$$\tau + \frac{(m+1)Q}{\lambda_0}\left(a\frac{r}{2} + B\frac{r^2}{3} + C\frac{r^3}{4} + D\frac{r^4}{5}\right) = \frac{C_1}{r},$$

where C_1 is the integration constant.

By returning to the variable U according to (A10), we find

$$\frac{\mathrm{d}U}{\mathrm{d}r} + \frac{(m+1)Q}{\lambda_0}\left(a\frac{r}{2} + B\frac{r^2}{3} + C\frac{r^3}{4} + D\frac{r^4}{5}\right) = \frac{C_1}{r}.$$

Boundary condition (A9) gives $C_1 = 0$ and

$$\mathrm{d}U + \frac{(m+1)Q}{\lambda_0}\left(a\frac{r}{2} + B\frac{r^2}{3} + C\frac{r^3}{4} + D\frac{r^4}{5}\right)\mathrm{d}r = 0.$$

By integrating this equality, we obtain

$$U + \frac{(m+1)Q}{\lambda_0}\left(a\frac{r^2}{4} + B\frac{r^3}{9} + C\frac{r^4}{16} + D\frac{r^5}{25}\right) = C_2, \tag{A11}$$

where C_2 is a constant. Then, we determine from boundary condition (A8) the constant

$$C_2 = U_\mathrm{w} + \frac{(m+1)Q}{\lambda_0}\left(a\frac{R_1^2}{4} + B\frac{R_1^3}{9} + C\frac{R_1^4}{16} + D\frac{R_1^5}{25}\right)$$

and, by substituting C_2 into (A11), we find

$$U(r) = U_\mathrm{w} + \frac{(m+1)Q}{\lambda_0}\left[\frac{a}{4}(R_1^2 - r^2) + \frac{B}{9}(R_1^3 - r^3) + \frac{C}{16}(R_1^4 - r^4) + \frac{D}{25}(R_1^5 - r^5)\right].$$

By using the change of variable (A6), we obtain the required solution (10)

$$T_\mathrm{g}(r) = \left\{T_1^{m+1} + \frac{(m+1)Q}{\lambda_0}\left[\frac{a}{4}(R_1^2 - r^2) + \frac{B}{9}(R_1^3 - r^3) + \frac{C}{16}(R_1^4 - r^4) + \frac{D}{25}(R_1^5 - r^5)\right]\right\}^{1/(m+1)}. \tag{10}$$

References

1. Sukhanov V.B., Fedorov V.F., Gubarev F.A., Tritskii V.O., Evtushenko G.S. *Kvantovaya Elektron.*, **37**, 603 (2007) [*Quantum Electron.*, **37**, 603 (2007)].
2. Shiyanov D.V., Evtushenko G.S., Sukhanov V.B., Fedotov V.F. *Kvantovaya Elektron.*, **37**, 49 (2007) [*Quantum Electron.*, **37**, 49 (2007)].

3. Vuchkov N.K., Temelkov K.A., Sabotinov N.V. *IEEE J. Quantum Electron.*, **41**, 62 (2001) [*Quantum Electron.,* **41**, 62 (2001)].
4. Vuchkov N.K., in *New Development in Lasers and Electric-Optics Research*. Ed. by W.T. Arkin (New York: Nova Sci. Publ. Inc., 2007) pp 41 – 74.
5. Carman R.J., Brown D.J.W., Piper A. *IEEE J. Quantum Electron.*, **30**, 1876 (1994).
6. Yakovlenko A.I. *Kvantovaya Elektron.*, **30**, 501 (2000) [*Quantum Electron.,* **30**, 501 (2000)].
7. Boichenko A.M., Evtushenko G.S., Zhdaneev O.V., Yakovlenko S.I. *Kvantovaya Elektron.*, **33**, 1047 (2003) [*Quantum Electron.,* **33**, 1047 (2003)].
8. Kushner M.J., Warner B.E. *J. Appl. Phys.*, **54**, 2970 (1983).
9. Astadjov D.N., Vuchkov N.K., Sabotinov N.V. *IEEE J. Quantum Electron.*, **24**, 1926 (1988).
10. Iliev I.P., Gocheva-Ilieva S.G., Sabotinov N.V. *Kvantovaya Elektron.*, **38**, 338 (2008) [*Quantum Electron.,* **38**, 338 (2008)].
11. Temelkov K.A., Vuchkov N.K., Pan B.L., Sabotinov N.V., Ivanov B., Lyutov L. *Proc. SPIE Int. Soc. Opt. Eng.*, **6604**, 660410-1 (2007).
12. Astadjov D.N., Dimitrov K.D., Jones D.R., Kirkov V.K., Little C.E., Sabotinov N.V., Vuchkov N.K. *IEEE J. Quantum Electron.*, **33**, 705 (1997).
13. Blau P., in *Pulsed Metal Vapour Lasers, NATO Science Partnership Sub-Series: 1, Vol. 5*. Ed. by C.E. Little, N.V. Sabotinov (New York: Springer, 1996) pp 215 – 220.
14. Jahnke E., Emde F., Losch F. *Tables of Higher Functions, 6th ed.* (New York: McGraw-Hill, 1960; Moscow: Nauka, 1977).